
ARTICLE

Applicability of a practical calibration for the small-type OSL dosimeter for measuring doses from direct X-rays and penetrating X-rays affected by scattered radiation

Tohru Okazaki^{a*}, Hiroaki Hayashi^b, Yoshiki Mihara^c, Takashi Asahara^c, Natsumi Kimoto^b, Yuki Kanazawa^c, Kosaku Higashino^c, Kazuta Yamashita^c, Sumi Yokoyama^d, Kazuki Takegami^c, Takuya Hashizume^{a, f}, Vergil Lorenzo E. Cruz^a and Ikuo Kobayashi^{a, g}

^aNagase Landauer, Ltd., Block C22-1, Suwa, Tsukuba, Ibaraki, 300-2686, Japan; ^bKanazawa University, 5-11-80 Kodatsuno, Kanazawa, Ishikawa, 920-0942, Japan; ^cGraduated School of Health Sciences, Tokushima University, 3-18-15 Kuramoto, Tokushima, Tokushima, 770-8503, Japan; ^dFUJITA HEALTH UNIVERSITY, 1-98 Dengakugakubo, Kutsukake-cho, Toyoake, Aichi, 470-1192, Japan; ^eYamaguchi University Hospital, 1-1-1, MinamiKogushi, Ube, Yamaguchi, 755-8505, Japan; ^fSOKENDAI, Shonan Village, Hayama, Kanagawa, 240-0193, Japan; ^gUniversity of Fukui, 1-3-33 Kanawa-cho, Tsuruga, Fukui 914-0055, Japan

A small type optically stimulated luminescence dosimeter, nanoDot, is expected to be applied to radiation dose evaluation on medical field. Dose calibration of a nanoDot is carried out by the air Kerma from incident X-ray generated by a diagnostic X-ray equipment. However the main component of exposure is not only direct X-ray beam but also scattered X-rays and penetrating X-rays. Therefore we evaluated the reliability of the dose calibration of nanoDot dosimeters on the exposure of different quality X-rays. The main calibration curve was determined by the air Kerma of 83 kV X-rays in the dose range of 3 μ Gy to 2 mGy. To validate the reliability of the calibration curve, the air kerma exposed to nanoDots and the response of nanoDots to scattered X-rays, penetrating X-rays and/or the entrance surface dose due to the 83 kV X-rays were evaluated. In the same manner, 55 and 108 kV X-rays were irradiated. The responses of nanoDots exposed by each condition were in good agreement with the main calibration curve and the reliability of it is $\pm 15\%$ even in 3 μ Gy. We concluded that the dose of diagnostic X-rays can be evaluated by the response of nanoDot calibrated by the air Kerma of 83 kV X-rays.

Keywords: OSL dosimeter; dose calibration; scattered X-ray; penetrating X-ray; diagnostic X-ray

1. Introduction

X-ray examinations are often applied to find tumors and various diseases in the human body. General X-ray photography is well known to be a quick and convenient method of examination; however, the exposure to diagnostic X-rays increases the risk of cancer [1]. In addition to the patient examination, X-rays are widely used to help the medical staff in surgical and other procedures such as interventional radiography. Currently, the effect of X-ray exposure to both patients and medical staff is an important topic [2,3], especially in the eye lens which is one of the most important doses being managed; to prevent cataracts, the International Commission on Radiological Protection (ICRP) recommended that the average value of an occupational exposure should be limited below 20 mSv during 5 years, with a maximum of 50 mSv per year [4]. There are some reports to estimate eye lens dose using optically stimulated luminescence dosimeter, thermoluminescence dosimeter, and/or radiophotoluminescent glass dosimeter worn close to the eye lens [5-8].

In order to manage X-ray exposure dose for patients and medical staff, we focused on a small-type optically stimulated luminescence (OSL) dosimeter called nanoDot [9-16]. The $10 \times 10 \times 2$ mm small type dosimeter is capable to evaluate the dose of a specific tissue. However, the energy dependence of nanoDot OSL dosimeter differs from tissue and the dosimeter does not have energy-compensation filters. Thus, it is essential to calibrate the dosimeter with a proper energy radiation source. Exposure doses to patients are mainly caused by direct X-rays generated by X-ray equipment, and doses to medical staff are due to scattered X-rays of which the X-ray spectra are different compared to direct X-rays. Therefore, it is important to consider the energy dependences of the dosimeter [9,10] to evaluate the doses for both patients and medical staff.

In a previous study, we proposed a unique calibration curve based on the air kerma of diagnostic X-rays, which can also evaluate the entrance skin dose (ESD) in the dose range of 0.3–6.0 mGy [16]. In this study, we enlarge the scope of the calibration curve not only for direct X-rays, but also for scattered and penetrating X-rays in a wider dose range. Additionally, we extended

*Corresponding author. Email: okazaki@nagase-landauer.co.jp

the lower limit of our calibration curve.

2. Materials and method

We used a nanoDot OSL dosimeter, made by Landauer, Inc. (Glenwood, Illinois, U.S.A.). The size of a nanoDot is 10 mm wide, 10 mm in length, and 2 mm thick. The detection component is $\text{Al}_2\text{O}_3:\text{C}$ and the effective density is 1.41 g/cm^3 [10]. Exposure dose to a nanoDot can be measured by using a portable measurement system; microStar reader (Landauer, Inc., Glenwood, Illinois, U.S.A.). When the detection component of a nanoDot is stimulated by green LED light, it emits blue luminescence. The amount of blue luminescence is proportional to the dose, thus, the microStar reader can evaluate the exposure dose by counting the luminescence using a photomultiplier tube. Each nanoDot has individual detection efficiencies ϵ which is determined by the manufacturer. To consider these differences, we used the values of counts/ ϵ , which were used in previous studies as well [14-16].

Diagnostic X-ray equipment (MRAD-A 50S/70, Toshiba Medical Systems Corporation, Otawara, Japan) was used to generate X-rays. We performed two experiments as shown in Figure 1. Setup A shows a free-air condition for direct X-ray exposure to the nanoDot. Setup B uses a phantom for direct X-ray exposure with scattered radiation, scattered X-rays, and penetrating X-rays with scattered radiation to the nanoDot. For setup A, the distance from the X-ray source to the dosimeter was set at 150 cm. For setup B, 20 cm thickness, 30 cm width, and 30 cm length of a soft-tissue-equivalent phantom (SZ-207, Kyoto Kagaku Ltd., Kyoto, Japan) was placed 150 cm away from the X-ray source. The irradiation area was $30 \text{ cm} \times 30 \text{ cm}$ on the incident surface of the phantom. Figure 1 represents the measurement points; (I) is the center of the beam axis for the detection of direct X-rays in free air condition; (II) is the center position at the front surface of the phantom for the detection of direct X-rays with scattered radiation (X-rays); (III) is located at 45° from the incident X-ray beam axis, 30 cm from the center of the phantom, for the detection of scattered X-rays; and (IV) is the center of the back surface of the phantom for the detection of penetrating X-rays with scattered radiation (X-rays). The ratio of air Kerma corresponding to (II)/(I) is known as the back scatter factor [17,18], and they were estimated to be between 1.3-1.4. At the measurement points (I), (II), (III), and (IV), a nanoDot or an ionization chamber was placed. The 3 cc thimble ionization chamber (DC300, PTW, Freiburg, Germany) calibrated by JQA was connected to an electrometer (EMF521, EMF Japan Ltd., Osaka, Japan). The air Kerma [J/kg] was derived by the measured value of ionization chamber. The uncertainty of this measurement system was approximately 5% ($k=2$) which is owed to the uncertainty of the calibration of the ionization chamber. Scattered X-rays generated by the movable diaphragm installed to the X-ray equipment [19] was negligibly small in the present experiment. The

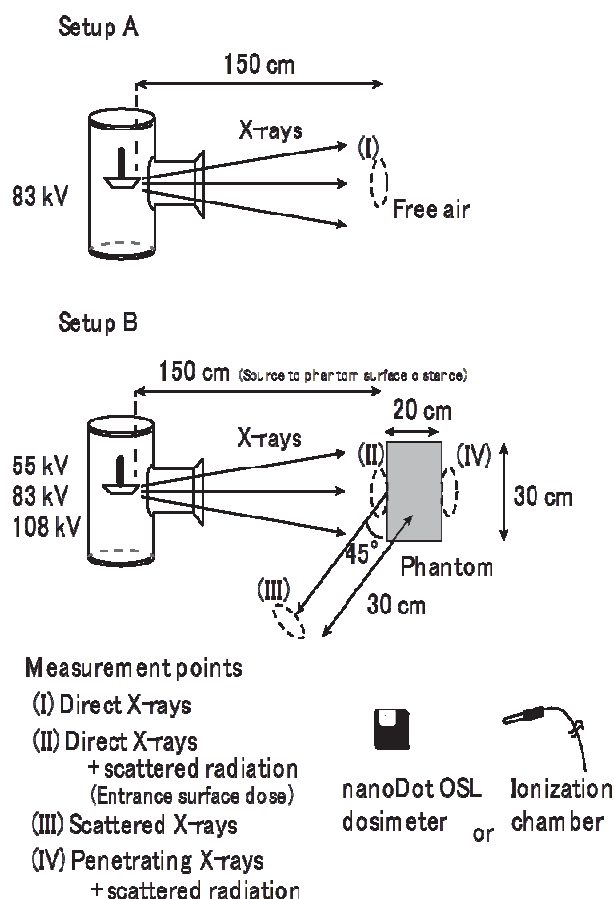


Figure 1. Schematic drawing of experimental set up using the nanoDot OSL dosimeter.

irradiation conditions are as follows. First, using 83 kV X-rays (half value layer (HVL) of 3 mm aluminum), data for direct X-rays under the conditions for position (I) shown in Figure 1 were measured; the tube-current-time products were set to 10 conditions between 0.5-200 mAs. Second, using 55 kV (HVL = 2 mm aluminum), 83 kV and 108 kV (HVL = 4 mm aluminum) X-rays, the data under the conditions for position (II), (III), and (IV) shown in Figure 1 were measured; the tube-current-time products were set to 6 conditions between 5-200 mAs. For each irradiation condition described above, measurements were carried out five times with the ionization chamber, and an average value of the air Kerma was adopted as reference data for the calibration. In contrast, for the nanoDot, irradiation was performed once for each of the irradiation conditions, and consecutive readings [20] were carried out five times using the reader.

3. Results

Figure 2 shows the relationship between air Kerma and counts/ ϵ measured with the nanoDot OSL dosimeter. The colored data shows present data including direct X-rays at 83 kV, direct X-rays with scattered radiation (ESD) at 55, 83, and 108 kV, scattered X-rays at 55, 83, and 108 kV, and penetrating X-rays with scattered radiation at 55, 83, and 108 kV. In this graph, the data of

55kV, 5 mAs in position (IV) were not presented because the relative uncertainties of them were over 100%. The solid line shows the proposed practical calibration curve determined by the data of 83 kV direct X-rays. The mathematical expression is as follows,

$$\frac{\text{Counts}}{\varepsilon} = 4638.2 \times \text{air Kerma [mGy]}. \quad (1)$$

The black dashed line in the upper figure shows the manufacturer's calibration data. These data are consistent with our experiment. The lower graph in Figure 2 shows deviations of data from the practical calibration curve. Although the response of nanoDot becomes higher in lower energy [15], the data are in good agreement with the curve in the energy range. The dashed line shows the relative uncertainty ($\pm 5\%$) of the calibration curve, which is estimated as described in the discussion (see Eq. (2)).

4. Discussion

We proposed a practical calibration curve using nanoDot OSL dosimeters without information about the irradiation conditions such as tube voltages (energy of X-rays). As described in a previous paper [16], the practical calibration curve has 15% uncertainty and the main elements were as follows: 1) systematic uncertainty caused by the individualities of the nanoDot OSL dosimeters $\sigma_{\text{sys}} = 5\%$, 2) an angular dependence of 5%, and 3) an energy dependence of less than 10%. Although Takegami made the above assumptions [16], there was no experimental evidence; it was unclear whether the practical calibration curve could be applied to measure air Kerma from direct X-rays with scattered radiation (ESD), scattered X-rays, and penetrating X-rays with scattered radiation. For the first time, the present study shows experimental evidence in support of this fact. Additionally, we extended the dose range of the practical calibration curve to 0.003 mGy from the previous reported value of 0.1 mGy [16]. A value of 0.003 mGy is obtained with the counts/ ε value of 10 and the statistical uncertainty of it becomes approximately 30%. Therefore when we use the practical calibration curve, we should take into account the statistical uncertainty of the counts/ ε value. The total uncertainty of the nanoDot is derived by the following formula,

$$\delta \frac{\bar{C}}{\varepsilon} = \frac{\bar{C}}{\varepsilon} \times \sqrt{\left(\frac{\delta \bar{C}}{\bar{C}}\right)^2 + (15\%)^2}, \quad (2)$$

Where \bar{C} indicates averaged value of counts.

One more new finding is that Landauer's calibration is consistent with the practical calibration curve we constructed.

The uncertainty value becomes approximately 15% at a dose range above 0.1 mGy, and it becomes worse at doses below 0.1 mGy because of the increasing statistical uncertainty. In the present study, we defined

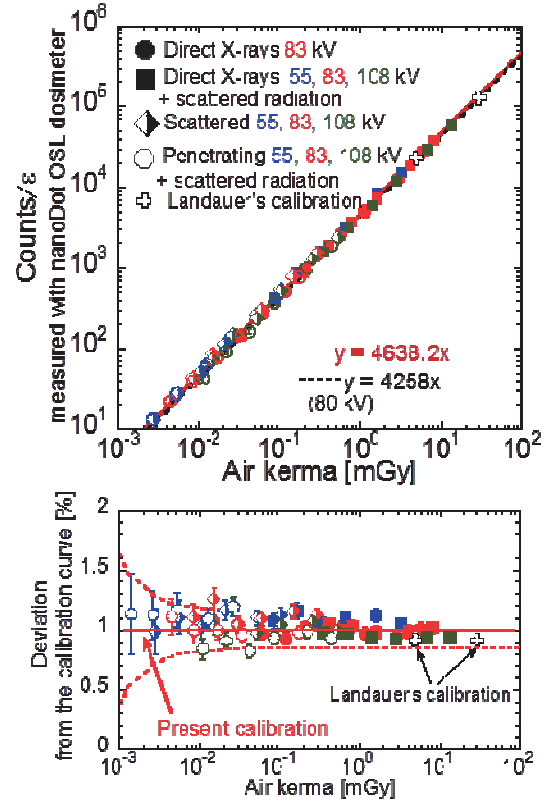


Figure 2. Experimentally determined calibration curve of the nanoDot OSL dosimeter. The data for direct X-rays, direct X-rays with scattered X-rays, scattered X-rays, and penetrating X-rays with scattered radiation are presented. Black data points represent the calibration points used for the microStar reader in default mode.

the lower detection limit as a dose at which relative uncertainty of it becomes 100%; it was estimated to be 5×10^{-4} mGy. In X-ray diagnosis, typical values of the entrance surface dose in medical examinations is estimated to be 0.2–7.8 mGy [21]. The detection limit (5×10^{-4} mGy) of the nanoDot was much smaller than that. Currently, some researchers recognize the importance of the management of exposure dose as well as image quality [22]. Therefore, we are involved in an effort to reduce radiation doses. The nanoDot is expected to be a suitable radiation detector.

5. Conclusion

We verified the applicability of a practical calibration curve for the nanoDot OSL dosimeter to measure the entrance surface dose (ESD), air Kerma of scattered X-rays, and penetrating X-rays with scattered radiation. The practical calibration curve was derived by the air Kerma of 83 kV diagnostic X-rays. By using a soft-tissue-equivalent phantom, the exposure conditions of ESD, scattered X-rays, and penetrating X-rays with scattered radiation were constructed. Then both the air kerma and the responses of nanoDot were measured. We concluded that these data were consistent with the practical calibration curve when adopting an additional uncertainty of 15%. Additionally, we evaluated the

lower detection limit of the measurement system to be 5×10^{-4} mGy.

Acknowledgements

This work was partially supported by JSPS KAKENHI Grant Number 15K19205.

References

- [1] A.B. Gonzalez and S. Darby, Risk of cancer from diagnostic X-rays: estimations for the UK and 14 other countries, *Lancet* 363 (2004), pp. 345-351.
- [2] T. Moritake, Y. Matsumaru, T. Takigawa et al., Dose measurement on both patients and operators during neurointerventional procedures using photoluminescence glass dosimeters, *American Society of Neuroradiology* 29 (2008), pp. 1910-1917.
- [3] A. Mohapatra, R.K. Greenberg, T.M. Masteacci et al., Radiation exposure to operating room personnel and patients during endovascular procedures, *Journal of Vascular Surgery* 58 (2013), pp. 702-709.
- [4] F.A. Stewart, A.V. Akleyev, M. Hauer-Jensen, et al., ICRP Statement on tissue reactions and early and late effects of radiation in normal tissues and organs-threshold doses for tissue reactions in a radiation protection context, *ICRP Publication* 118, ICRP (2012).
- [5] R.M. Sanchez, E. Vano, J.M. Fernandez, et al., Measurements of eye lens doses in interventional cardiology using OSL and electronic dosimeters, *Radiation Protection Dosimetry* 162(4) (2014), pp. 569-576.
- [6] E. Carinou, M. Brodecki, J. Domienik, et al., Recommendations to reduce extremity and eye lens doses in interventional radiology and cardiology, *Radiation Measurement* 46 (2011), pp. 1324-1329.
- [7] F. Vanhavere, E. Carinou, G. Gualdrini, et al., Optimization of radiation protection of medical staff, EURADOS report 2012-02, EURADOS (2012).
- [8] A. Hirakuri, K. Numasawa, H. Takeishi, et al., Study of radiation dose to the eye lens by multi-detector row computed tomography of the temporal bone, *Japanese Journal of Radiological Technology* 68(6) (2012), pp. 720-725.
- [9] R.M. Al-Senan and M.R. Hatab, Characteristics of an OSLD in the diagnostic energy range, *Medical Physics* 38 (2011), pp. 4396-4405.
- [10] J.R. Kerns, S.F. Kry, N. Sahoo et al., Angular dependence of the nanoDot OSL dosimeter, *Medical Physics* 38 (2011), pp. 3955-3962.
- [11] P.A. Jursnic, Characterization of optically stimulated luminescence dosimeters, OSLDs, for clinical dosimetric measurements, *Medical Physics* 34 (2007), pp. 4594-4604.
- [12] J. Lehmann, L. Dunn, J.E. Lye et al., Angular dependence of the response of the nanoDot OSLD system for measurements at depth in clinical megavoltage beams, *Medical Physics* 41 (2014), 061712 (9 pages).
- [13] K. Takegami, H. Hayashi, H. Okino et al., Estimation of identification limit for a small-type OSL dosimeter on the medical images by measurement of X-ray spectra, *Radiological Physics and Technology* 9 (2016), pp. 286-292.
- [14] H. Hayashi, K. Takegami, H. Okino et al., Procedure to measure angular dependences of personal dosimeters by means of diagnostic X-ray equipment, *Medical Imaging and Information Science* 32 (2015), pp. 8-14.
- [15] K. Takegami, H. Hayashi, H. Okino et al., Energy dependence measurement of small-type optically stimulated luminescence (OSL) dosimeter by means of characteristic X-rays induced with general diagnostic X-ray equipment, *Radiological Physics and Technology* 9 (2016), pp. 99-108.
- [16] K. Takegami, H. Hayashi, H. Okino et al., Practical calibration curve of small-type optically stimulated luminescence (OSL) dosimeter for evaluation of entrance skin dose in the diagnostic X-ray region, *Radiological Physics and Technology* 8 (2015), pp. 286-294.
- [17] H. Kato, Method of calculating the backscatter factor for diagnostic X-rays using the differential backscatter factor, *Japanese Journal of Radiological Technology* 57(12) (2001), pp. 1503-1510.
- [18] H. Kato, K. Minami, Y. Asada, et al., Analysis of scattered radiation in an irradiated body by means of the Monte Carlo simulation: Back-scatter factors of diagnostic X-rays in the incident surface which is not flat, *Japanese Journal of Radiological Technology* 72(5) (2016), pp. 396-401.
- [19] I. Maehata, H. Hayashi, N. Kimoto et al., Practical method for determination of air kerma by use of an ionization chamber toward construction of a secondary X-ray field to be used in clinical examination rooms, *Radiological Physics and Technology* 9 (2016), pp. 193-201.
- [20] H. Hayashi, K. Nakagawa, H. Okino, et al., High accuracy measurements by consecutive readings of OSL dosimeter, *Medical Imaging and Information Science* 31(2) (2014), pp. 28-34.
- [21] Y. Matsunaga, A. Kawaguchi and K. Kobayashi, Dose estimation for exposure conditions of diagnostic radiology acquired by a 2011 questionnaire in a phantom study, *Japanese Journal of Radiological Technology* 69(12) (2013), pp. 1372-1378.
- [22] M. Uffmann and C. Schaefer-Prokop, Digital radiography: The valance between image quality and required radiation dose, *European Journal of Radiology* 72 (2009), pp. 202-208.